A Novel Realistic Simulation Framework for Rigorous Validation of Insulin Therapies: Integrating Stochastic and Data-Driven Variability

Xiomara Rodríguez-Sarmiento[a], David L. Rodríguez-Sarmiento[b], Maira García-Jaramillo[c], Leonel Paredes-Madrid[a], Fabian León-Vargas[a,*]

[a]*Facultad de Ingeniería Mecánica, Electrónica y Biomédica, Universidad Antonio Nariño, Bogotá D.C., Colombia.*
[b]*Vicerrectoría de investigación, Universidad Manuela Beltrán, Bogotá D.C., Colombia*
[c]*Facultad de Ingeniería, Universidad Ean, Bogotá D.C., Colombia*

Abstract

Preclinical evaluations of glycaemic control algorithms often rely on simulators that underestimate real-world metabolic variability, leading to overly optimistic performance. A novel type 1 diabetes (T1D) simulation framework, DT1-UAN v2, was developed to generate physiologically realistic and adaptive scenarios for an improved assessment of insulin therapies. DT1-UAN v2 integrates two disturbances of intrapatient variability: eight, stochastically parameterised insulin sensitivity (S_I) patterns and sixty data-driven profiles for the rate of blood glucose appearance (R_a). Incorporating these features exposed vulnerabilities in insulin therapies that previously relied on static physiological parameters. In-silico trials on virtual T1D subjects, under both open- and closed-loop therapies, revealed contrasts between outcomes obtained with DT1-UAN v2 and the earlier DT1-UAN v1. Control strategies that appeared effective in static scenarios often produced different results in the enhanced framework, uncovering underestimated risks of post-prandial hypoglycaemia or sustained hyperglycaemia. These findings demonstrate that incorporating realistic S_I and R_a variability is essential for rigorous preclinical testing, as simplified models can conceal clinically relevant risks. The proposed framework provides a valuable tool for identifying hidden design flaws and enabling the development of more adaptive, and safer control strategies for people with T1D. This enhanced realism provides a critical foundation for testing and optimising personalised insulin treatments.

Keywords: artificial pancreas, insulin sensitivity, rate of blood glucose appearance, realistic simulation, type 1 diabetes

*Corresponding author.
Email addresses: Xrodriguez67@uan.edu.co (Xiomara Rodríguez-Sarmiento), David.RodriguezS@docentes.umb.edu.co (David L. Rodríguez-Sarmiento), magarcia@universidadean.edu.co (Maira García-Jaramillo), paredes.leonel@uan.edu.co (Leonel Paredes-Madrid), fabianleon@uan.edu.co (Fabian León-Vargas)

1. Introduction

Type 1 diabetes (T1D), a chronic autoimmune disease requiring intensive insulin therapy [1], is increasingly managed using automated insulin delivery (AID) systems [2–5]. Over the past two decades, the development of these closed-loop control (CLC) systems has been significantly accelerated by in-silico simulators, which provide a platform for preclinical testing [6, 7]. As noted in a recent state-of-the-art review by Cinar et al. [8], these simulators are the critical foundation for the next frontier in personalized medicine: the Digital Twin. However, the clinical utility of any digital twin is directly limited by the realism of its underlying simulation engine. A fundamental gap persists, as many current simulators, including the FDA-accepted UVA/Padova simulator [9–11], still operate under idealized conditions with static parameters, limiting their predictive power.

Control algorithms validated in such static environments may exhibit unexpectedly poor performance when faced with real-world metabolic variability, leading to systematically biased conclusions [12–18]. Two of the most challenging disturbances for any CLC algorithm are the daily fluctuations in insulin sensitivity (S_I) and the highly variable rate of glucose appearance (R_a) from meals [18–20]. While some simulators have addressed these factors in isolation [21–25], a unified framework that integrates both empirically derived R_a profiles and stochastic S_I dynamics has been lacking. Indeed, the library of glucose absorption profiles used in this work, previously developed in [26], has already been employed by other research groups to validate virtual patient models in the context of Digital Twins [27], underscoring the need for increasingly realistic simulation tools.

To address this critical gap, this work presents the DT1-UAN v2: a significantly updated T1D simulation framework designed to challenge glycaemic control algorithms with a more faithful representation of intrapatient variability. The framework introduces two key architectural innovations: the integration of eight stochastically parameterized S_I patterns and a comprehensive library of sixty data-driven R_a profiles. This dual focus on both low-frequency disturbances (circadian sensitivity) and high-frequency disturbances (meal digestion) provides a more stringent and versatile testbed for the preclinical evaluation of insulin therapies, enabling the development of more robust and adaptive control strategies for people with T1D.

2. Methods

2.1. Stochastic Insulin Sensitivity Dynamics

To implement intrapatient variability, eight patterns of S_I were considered, based on a systematic protocol proposed by Visentin et al. [20], included in the UVA/Padova simulator [28]. These patterns were extracted based on data from a clinical study conducted in 20 PWT1D patients following a mixed diet protocol. Blood samples were analysed three times a day to measure glucose and insulin levels, leading to the identification of eight daily patterns of S_I considering normalisation and classification processes.

2.1.1 Definitions

These S_I patterns represent simplified categorization of circadian insulin sensitivity profiles, where each day is divides intro three-time intervals: breakfast (B) from 04:00 to 11:00 h, lunch (L) from

11:00 to 17:00 h, and dinner (D) from 17:00 to 04:00 h. Each step of the S_I pattern was categorized as either level "high" (h) or "low" (l) depending on whether the assigned S_I value is above or below the subject's daily basal average. This results in codified patterns such as h-h-l or l-h-h, where each letter indicates the S_I level during B, L, and D, respectively (see Table 1). The S_I values assigned according to the β for high level and α for low level parameters, respectively. Unlike the approach proposed by Visentin et al. [20], where β and α were fixed at 1.0 and 0.4, respectively. A random value into the ranges $1 \leq \beta \leq 2$ and $0.1 \leq \alpha \leq 1$ was assigned to allow stochastic testing scenarios using the same virtual subject

Additionally, each value (either β or α) was slightly modulated by a random variable γ, sampled from a normal distribution with $\mu = 1$ and $\sigma = 0.2$ (see Eq. 1) following [20]. This modulation occurs through a multiplicative effect, where the assigned SI value is scaled by γ. As a result, even for the same classification (high or low), the final value varies across different steps. To ensure smooth transitions between steps in the S_I pattern, cubic interpolation was applied during transition periods: from 2:30 h to 5:30 h, from 9:30 h to 12:30 h, and from 16:00 h to 19:00 h each day. This method was chosen to ensure a continuous transition between sensitivity levels, avoiding the physiologically unrealistic sharp changes that could introduce simulation artifacts. Figure 1 presents examples of S_I pattern realizations.

$$\gamma = N(\mu, \sigma^2) \quad (1)$$

Table 1. Stepwise approach of the insulin sensitivity (S_I) patterns proposed by Visentin et al. [20], where 'h' denotes high and 'l' denotes low, and β and α are their assigned values.

#	**S_I Patterns Breakfast-Lunch-Dinner**	
	Level	Value
1	*h-h-h*	β-β-β
2	*h-h-l*	β-β-α
3	*h-l-h*	β-α-β
4	*h-l-l*	β-α-α
5	*l-h-h*	α-β-β
6	*l-h-l*	α-β-α
7	*l-l-h*	α-α-β
8	*l-l-l*	*α-α-α*

Figure 1 (left) illustrates one possibility of patterns 2, 4, and 7 from Table 1, providing a visual representation of the above definition. Figure 1 (right) compares one possibility of pattern 2 before (blue dashed line) and after incorporating random variations of Eq. 1 (blue solid line).

Notably, even when two steps are classified as "high" (h), their values may differ due to the multiplicative effect of the random variable γ. For instance, in Figure 1 (right) the breakfast interval, the variation is 0.97, whereas in the lunch interval, it is 1.13. This means that despite having multiple

occurrences of "h" or "l" in a pattern, their specific values depend on the scaling effect introduced by γ. Depending on the magnitude of this variation, the difference between "l" and "h" may be substantial or minimal, as observed in Figure 1.

2.2.2 *Implementation*

The glucose–insulin model developed by Dalla Man et al. [25], and employed in DT1-UAN v1 [13] (Appendix A), describes that insulin-dependent glucose utilisation (U_{id}) and endogenous glucose production (EGP) depend on the rate of glucose utilisation by tissues (V_{mx}) and the rate of glucose production by the liver (k_{p3}), respectively, affecting the blood insulin concentration (Eq. A.20 – Eq. A.27). Therefore, U_{id} and EGP depend on S_I. To achieve a realistic variation in U_{id} and EGP, V_{mx} and k_{p3} should vary over time following a specific S_I pattern and its corresponding "high" and "low" levels. Making these parameters vary over time allows for more realistic behaviour for a cohort of virtual subjects [20]. In this way, insulin sensitivity is modified, and its effect will be evaluated compared to a so-called Pattern 0 without variation of DT1-UAN v1; this comparison is later shown in Section 3 of this manuscript.

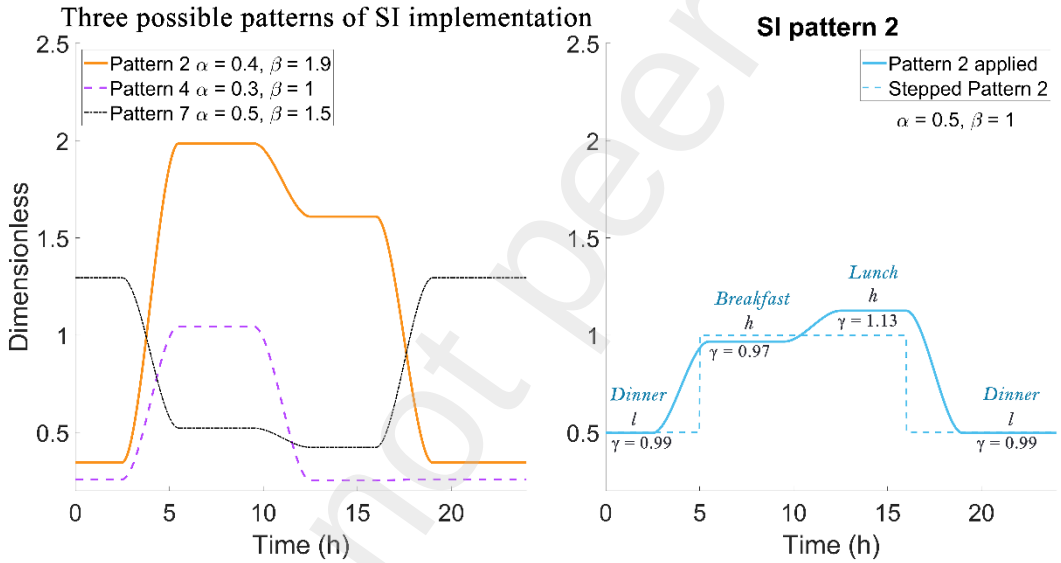

Figure 1 Twenty-four-hour of smoothed S_I patterns. Left: pattern 2 with β = 1.9 and α = 0.4 (orange solid line), pattern 4 with β = 1 and α = 0.3 (purple dashed line), and pattern 7 with β = 1.5 and α = 0.5 (black dotted line). Right: smoothed pattern 2 with β = 1 and α = 0.5 (solid line) and its primary stepped pattern (dashed line)

2.2. Data-Driven *Meal* Absorption Library

To incorporate realistic dynamics of R_a into the DT1-UAN v1 simulator, a library of sixty data-based profiles representing several conventional (daily-life) meals was adapted from the MICELab group works [26]. This library was built using Bayesian identification methods from clinical study data [29, 31]. Each meal includes the meal composition, ingredients, and the corresponding Ra profile labelled as Cn, where n represents the meal ID number.

The library includes the meal composition of fat, protein, fibre, energy, and carbohydrate (CHO) content. They are categorised as “large”, “medium”, “small”, or “fast” based on their absorption speed and glycaemic index. This provides valuable information on how each meal can affect postprandial blood glucose (BG) levels. Examples of a conventional meal of each category are illustrated in Figure 2a. Meals with a low glycaemic index produce a slower and more sustained BG response, and conversely, meals with a high glycaemic index are rapidly absorbed and lead to a quick increase in BG levels, making them useful as a source of quick energy in cases of hypoglycaemia [30].

Each data-based R_a profile in this library consists of 85 values representing samples every 5 minutes, which corresponds to 7 hours from the start of meal consumption. When a meal ID is chosen, the corresponding data-based R_a profile is retrieved from the library, and a linear interpolation is used to obtain samples every minute. To smooth out the tail of each profile and avoid a sudden ending at zero after the 7 hours, cubic interpolation is applied in the realization (see Figure 2a). This approach ensures a gradual and physiologically plausible decline to baseline, preventing an abrupt termination of glucose absorption that would not occur in reality. This ensures a gradual decline in R_a values until they reach zero, adding approximately 2 additional hours to the signal. Consequently, the total duration of the R_a profile extends to approximately 9 hours, allowing a more physiologically realistic transition to baseline.

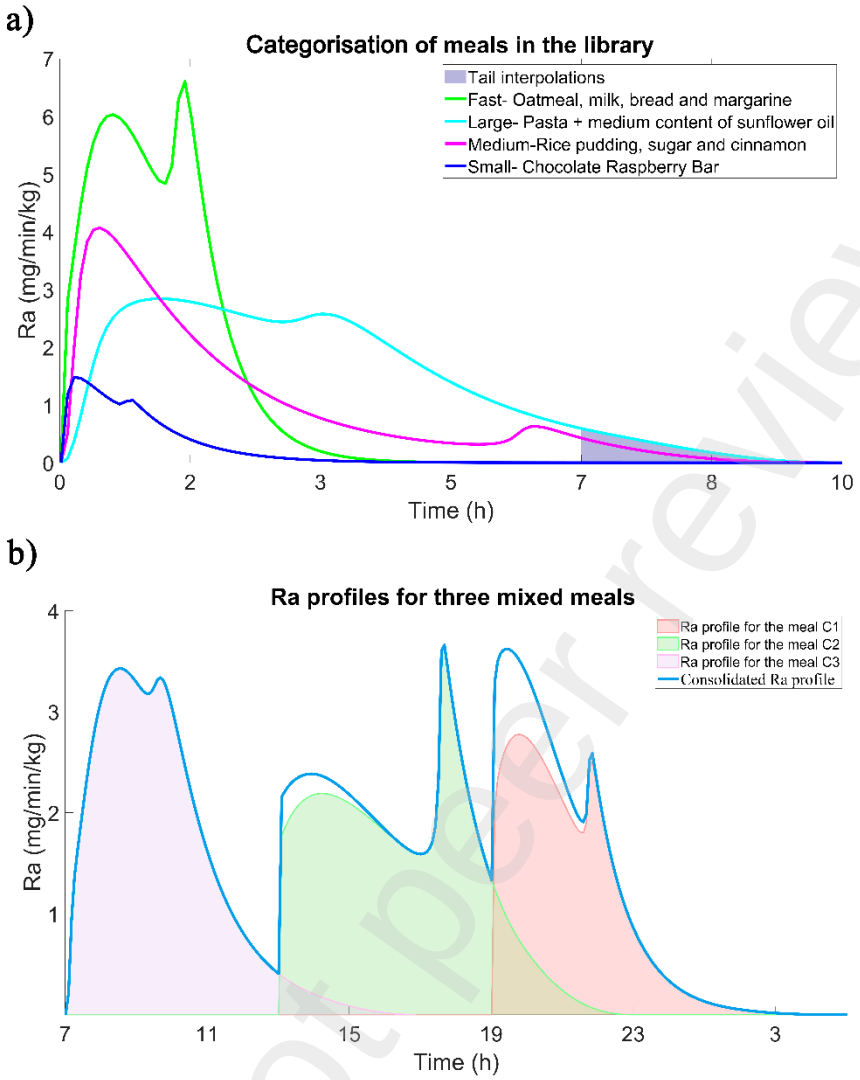

Figure 2 a. Representation of the rate of blood glucose appearance of conventional meals from each category considered in the library: "large" (cyan), "medium" (pink), "small" (blue), and "fast" (green), along with the corresponding tail interpolations (shadowed). **b.** Consolidated trace of the R_a profile (blue). Individual R_a traces (C1 at 7:00 h, C2 at 13:00 h and C3 at 19:00 h) merged in a unique trace

In case of a simulation involving multiple meals, the corresponding R_a profiles are retrieved and applied according to the consumption timing schedule of the in-silico test. When two profiles intersect, they are combined by summing up their values at each time point to generate a single data-based R_a profile. Subsequently, this profile is multiplied by the fraction of absorbed carbohydrates (f parameter) and divided by the patient's weight in kilograms (W) (see Eq. 2).

$$R_a(t) = f_a \times \text{data - based } R_a\, profile\,(t) \times \frac{f}{w} \qquad (2)$$

Thus, each virtual subject implements a personalized data-based R_a profile according to its particular physiological characteristics. This procedure is consistent with the one employed in the carbohydrate absorption model implemented by the UVA/Padova simulator [12, 28].

September 5, 2025

Figure 2 b shows the consolidated data-based R_a profile and the corresponding individual profiles for three meals: C1 "Standard breakfast" of 70.3 g CHO at 7:00 h; C2 "Pasta with high sunflower oil content" of 75 g CHO at 13:00 h; and C3 "Pasta with tomato sauce" of 50 g CHO at 19:00 h.

According to [22], the area under the curve (AUC) of R_a (see Eq. 3) indicates how many carbohydrates of the ingested meal D are transported from the intestine to the blood during time T (min) considering the fraction of carbohydrates absorbed associated to the *f* parameter.

$$\int_0^T R_a(t)dt = fD \quad (3)$$

However, unlike the R_a profile obtained using the carbohydrate absorption model in the UVA/Padova simulator, the amount of carbohydrates absorbed in each conventional meal from the library [22, 29] did not fully align with Eq. 3, resulting in an average percent error of 10.17% ± 0.102.

To address this discrepancy, a systematic adjustment factor (f_a) was derived to align the data-based profiles with the total expected glucose absorption. For each of the 60 profiles, the AUC of the data-based R_a was calculated. This value was then compared to the theoretical total absorbed carbohydrates (fD, from Eq. 3). The ratio of the theoretical amount to the data-derived AUC was computed for each meal, and the average of these 60 ratios yielded the final adjustment factor, f_a =1.10165. Applying this uniform scaling factor to all profiles in the library systematically corrects for the average discrepancy in the original dataset. This reduced the average percent error to 1.33% ± 0.007 [31] (see Eq. 2).

3. Results

3.1 Evaluating the new realistic features of the simulator

To evaluate the new realistic behaviour of virtual subjects, namely, patterns of insulin sensitivity S_I and data-based profiles of conventional R_a, four in-silico tests were conducted. These tests were divided into two groups to address separate realistic effects. The first one includes three tests, and the second one includes one test. Each test is detailed as follows.

In the first group, all tests were performed on a single virtual adult subject available in the commercial version of the UVA/Padova simulator (Section 4.1), over a 24-hour scenario to evaluate the effects of both the S_I and R_a profiles. According to [12], this virtual subject has a weight of 80.34 kg, k_{p3} of 0.0118 mg/kg/min per pmol/litre, V_{mx} of 0.1297 mg/kg/min per pmol/litre, and an optimal basal insulin of 1.39 IU/h. Each test was designed to evaluate both individual and combined behaviour with and without the implemented features.

The first test examined the effect of different S_I patterns on the subject's glycaemia excursions. The second one, examined the effect of using a library of conventional meals compared to meals from the model-based UVA/Padova simulator; that is, data-based vs model-based R_a profiles. Finally, the third test examined the accumulated effects on glucose and insulin concentrations under OLC and CLC therapies.

The fourth test, belonging to the second group, was conducted exclusively in CLC over 24 hours on the complete cohort of adult virtual subjects available in the commercial version of the UVA/Padova simulator (Section 4.2). Adult #007 was excluded due to unrealistic characteristics [32]. In this test, both features were employed simultaneously, thus evaluating the simulator's behaviour for a group of subjects in a test for insulin therapy.

The OLC therapy considered was based on a constant rate of basal insulin infusion, optimised for each subject, no correction bolus, and specific boluses based on the 1700 rule. This rule is computed automatically in the UVA/Padova simulator and was based on the carbohydrate factor (CF), carbohydrate rate (CR), and the total daily insulin (TDI) estimated from basal infusion and CR [28].

The CLC therapy considered was based on the PD-basal controller used in [15], which employs a fully automated insulin infusion system with a glycaemic target of 120 mg/dL. It provides insulin doses proportionally to the BG levels and to the rate of change of these levels. Unlike a PID controller, the PD-basal controller does not employ an integral action but a constant basal insulin to correct steady-state error. No additional safety systems were implemented.

3.1.1 Evaluations in a single *adult* virtual subject

Behaviour of circadian variation in insulin sensitivity

For illustrative reasons, S_I patterns 2, 4, and 7 (Table 1) were chosen to observe their effect on glucose with respect to no variations in S_I (pattern 0 of DT1-UAN v1), see Figure 1. A constant basal rate of insulin was administered without meals. Figure 3 shows the BG levels obtained after implementing each S_I pattern. The first row shows the outcome when S_I pattern 0 is used, followed by realistic patterns: S_I pattern 2 with $\beta = 1$ and $\alpha = 0.5$ (second row), S_I pattern 2 with $\beta = 1.9$ and $\alpha = 0.4$ (third row), S_I pattern 4 with $\beta = 1$ and $\alpha = 0.3$ (fourth row), and S_I pattern 7 with $\beta = 1.5$ and $\alpha = 0.5$ (last row).

When using S_I pattern 0 glucose remains constant at 120 mg/dL (glycaemic target by default), however under S_I pattern 2, 4 and 7 glucose tends to fluctuate between 81.84 mg/dL and 155.85 mg/dL, depending on the case. These fluctuations allude to the patient experiencing variations on insulin sensitivity, leading to lower glucose levels around 80 mg/dL, or, conversely, resulting in higher BG levels.

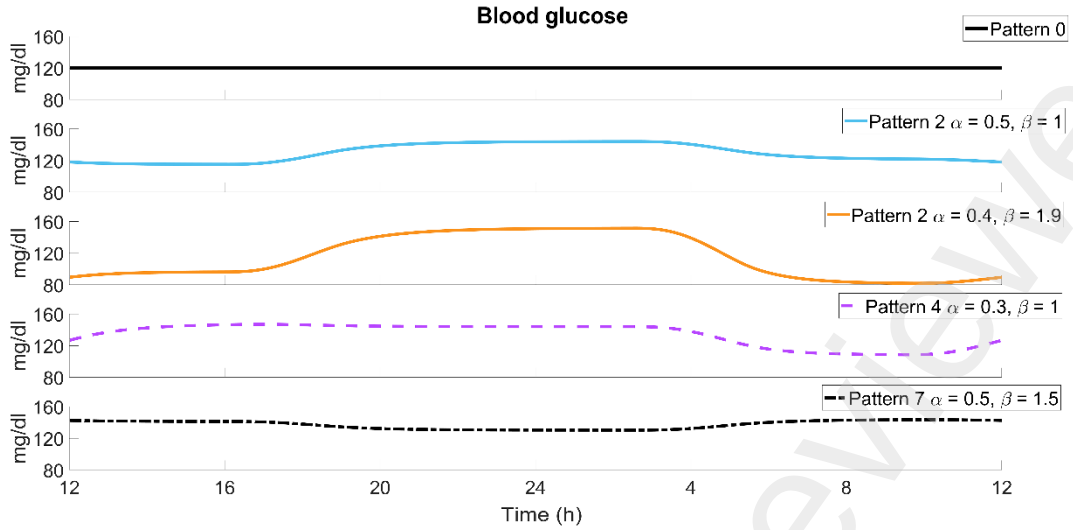

Figure 3 Blood glucose levels obtained over 24 hours under several S_I patterns for a virtual subject using the same constant basal insulin in all cases

Behaviour of realistic profiles of the Rate of glucose appearance

Regarding the impact of the library of conventional meals, the adult virtual subject was simulated from 11:00 h to 18:00 h in two scenarios integrating data-based and model-based R_a profiles, respectively. These interventions were conducted using an OLC therapy with a predefined CF for each meal and the S_I pattern 0 (without variation).

In the first scenario (data-based R_a profile), the meal plan comprised lunch (spaghetti with tomato, cheese, and lentils, totalling 87 g of CHO) classified as "fast" and ingested at noon; dinner (baked potato, gelatine, and turkey breast, totalling 45 g of CHO) classified as "medium" and ingested at 22:00 h; and finally, a dessert (biscuit with fat-free yoghourt, totalling 94 g of CHO) classified as "large" and ingested at 17:00 h. The second scenario (model-based Ra profile) used the carbohydrate absorption model implemented in the UVA/Padova simulator, the same as DT1-UAN v1, using identical amounts of CHO.

Figure 4 presents the R_a profiles and corresponding BG traces obtained with the library of conventional meals (data-based) and with the original UVA/Padova simulator meals (model-based). While model-based R_a profiles showed consistent dynamics that varied only in proportion to the amount of CHO, with most of the carbohydrates being absorbed at the beginning of meal ingestion, data-based R_a profiles exhibited a prominent variability. For example, the first meal, a "fast" one profile, is absorbed quickly over time, while the second meal, a "medium" one profile, shows a meal absorption prolonged over time. An increased risk of hypoglycaemia was ultimately observed with the data-based R_a profiles.

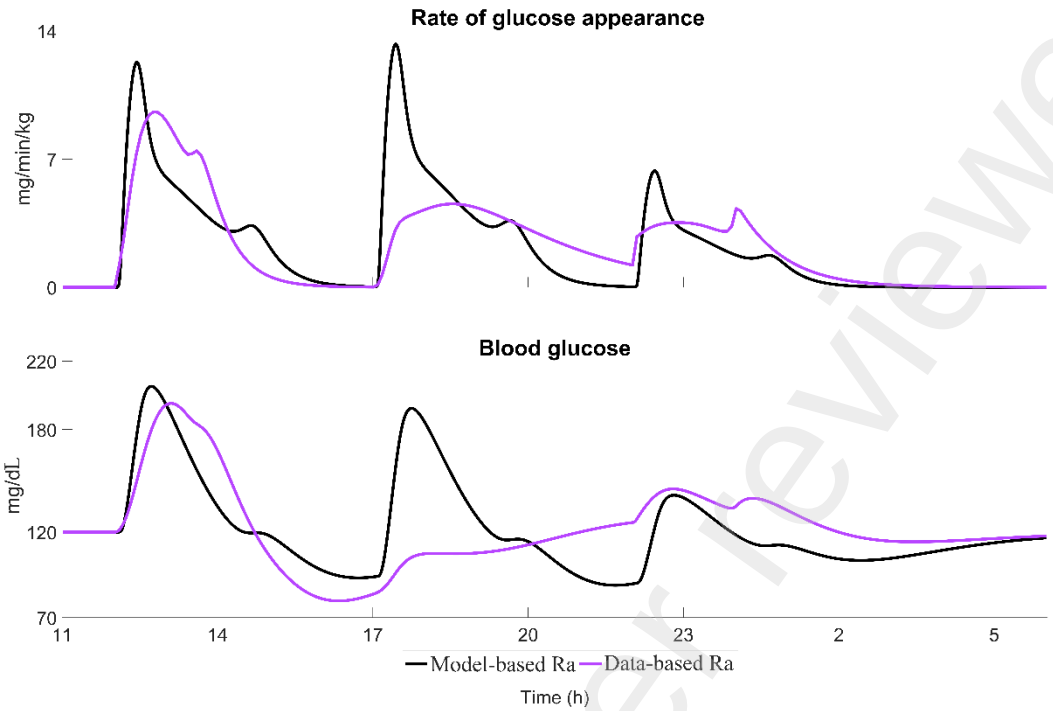

Figure 4 Blood glucose comparison between data-based and model-based R_a profiles. Above the model-based (black line) and data-based (purple line) R_a profiles, and below the corresponding blood glucose concentration of a subject under the same open-loop therapy.

Behaviour of combined effects

In this test, both OLC and CLC therapies were implemented over 24 hours. The in-silico trial started at 15:00 h, and S_I pattern 2 with $\beta = 1$ and $\alpha = 0.5$ was used. In case of realistic meals (data-based R_a profiles), plan consisted of lunch - boiled rice, corn, and turkey breast - comprising 50 g of CHO at 16:00 h, and dinner - pasta, tomato sauce, oil, and psyllium - comprising 50 g of CHO at 22:00 h. Both meals are classified as "medium" in the library. In case of model-based R_a profiles, meals of 50 g were considered for consistency.

Four scenarios were considered: "data-based R_a profile with S_I pattern 2", "data-based R_a profile with S_I pattern 0", "model-based Ra profile with S_I pattern 2", and "model-based R_a profile with S_I pattern 2". Results are depicted in Figure 5, showing the BG response and insulin infusion using OLC and CLC insulin therapies in each scenario.

Figure 5a depicts the rate of glucose appearance related to both meals of 50 g CHO ingested at 16:00 h and 22:00 h. Figure 5b shows the insulin sensitivity of S_I pattern 0 and 2. Figure 5c and 5E show the insulin infusion rates resulting from the OLC and CLC therapies applied. Finally, Figure 5d and 5f show the BG concentrations under OLC and CLC therapies, respectively.

Regarding the OLC therapy, a basal insulin concentration of 1.4 IU/h remained unchanged along with two identical prandial boluses, each of 4.13 IU. Conversely, the CLC exhibited varying insulin delivery rates. In "model-based R_a profile with S_I pattern 0" scenario, insulin peaks of 9.8 IU/h were

observed in both meals followed by insulin suspensions (0 IU/h) lasting approximately two hours. A similar behaviour was observed in "model-based R_a profile with S_I pattern 2" scenario.

On the other hand, postprandial insulin peak rates of 4.6 IU/h vs. 4.6 IU/h and 3.6 IU/h vs. 3.8 IU/h (approximately half of the value obtained with conventional meals), were observed in "data-based R_a profile with S_I pattern 0" and "data-based R_a profile with S_I pattern 2" scenarios, respectively. Consequently, shorter periods of insulin suspension were obtained with respect to model-based R_a cases.

The resulting glycaemic traces show that the waveform of the postprandial BG response was substantially altered by the different scenarios. As seen in Figure 5d and 5f, under both OLC and CLC, the "model-based R_a with S_I pattern 0" scenario resulted in sharp postprandial peaks that returned towards the baseline relatively quickly. In contrast, the scenarios incorporating data-based R_a profiles led to broader, and in some cases, delayed glycaemic excursions. Specifically, under CLC (Figure 5f), the combination of "data-based R_a with S_I pattern 2" resulted in a prolonged period of hyperglycaemia after the second meal, a behaviour not observed in the simplified scenario. This demonstrates a marked difference in the closed-loop system's observed performance that is dependent on the level of realism incorporated into the simulation.

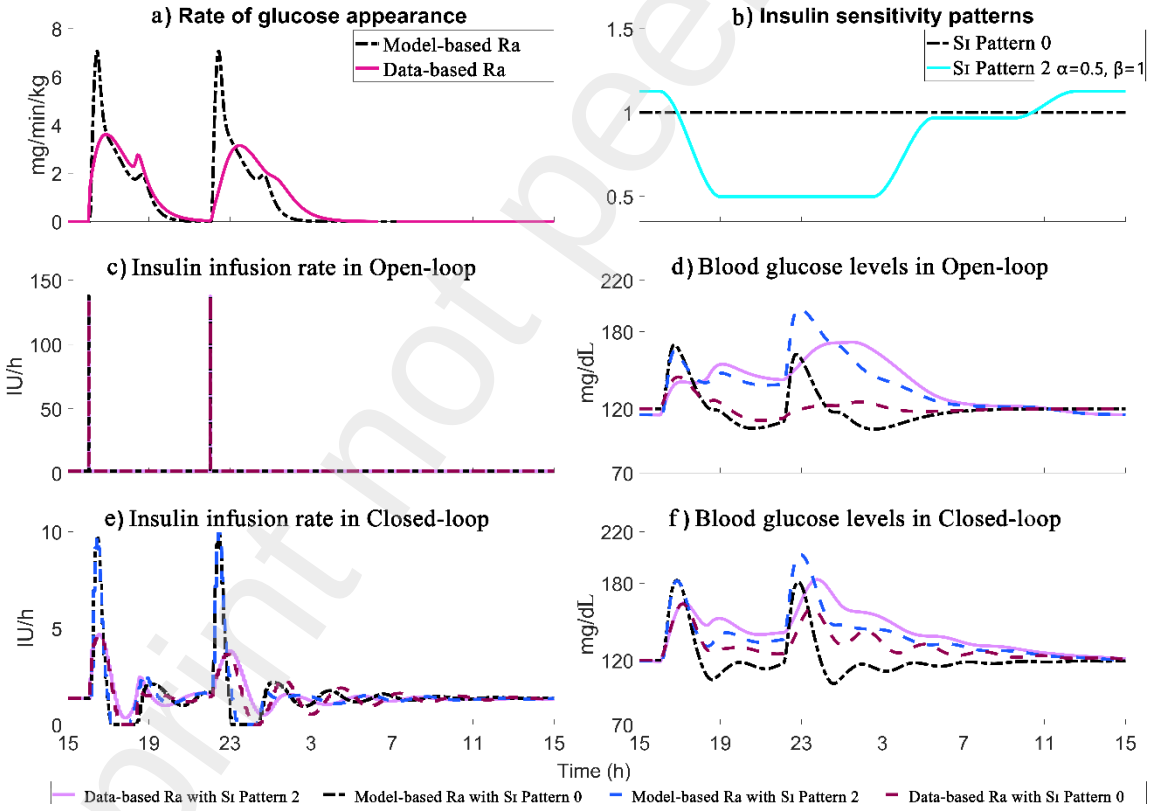

Figure 5 Study results for "data-based R_a profile with S_I pattern 2", "model-based R_a profile with S_I pattern 0", "model-based R_a profile with S_I pattern 2", and "data-based R_a profile with S_I pattern 0". **a)** Data-based and model-based R_a profiles. **b)** S_I patterns 0 (constant) and 2 (variable). **c)** Open-loop insulin infusion rates. **d)** Open-loop blood glucose levels. **e)** Closed-loop insulin infusion rates. **f)** Closed-loop blood glucose levels

September 5, 2025

Evaluation in a cohort of virtual subjects

In this test, two scenarios using the same CLC therapy for 24 hours beginning at 7:00 h were implemented over the cohort of 10 adult virtual subjects. The first one included data-based R_a profile with S_I pattern 2 with $\beta = 1$ and $\alpha = 0.5$, and the second included model-based R_a profile with S_I pattern 0 (no variations).

The meal plan consisted of breakfast - oat cereal, milk, strawberry jam, and orange juice - classified as "medium" and comprising 69 g of CHO at 7:00 h, followed by lunch - pasta with a high content of sunflower oil - classified as "large" comprising 75 g of CHO at 13:00 h, and finally, dinner - pasta and tomato sauce - classified as "medium" comprising 50 g of CHO at 19:00 h. In case of model-based R_a profiles, identical amounts of CHO at the same timing were used. Figure 6 shows the results obtained. Additionally, Table 2 presents a comparison of several glycaemic control indicators computed from this test.

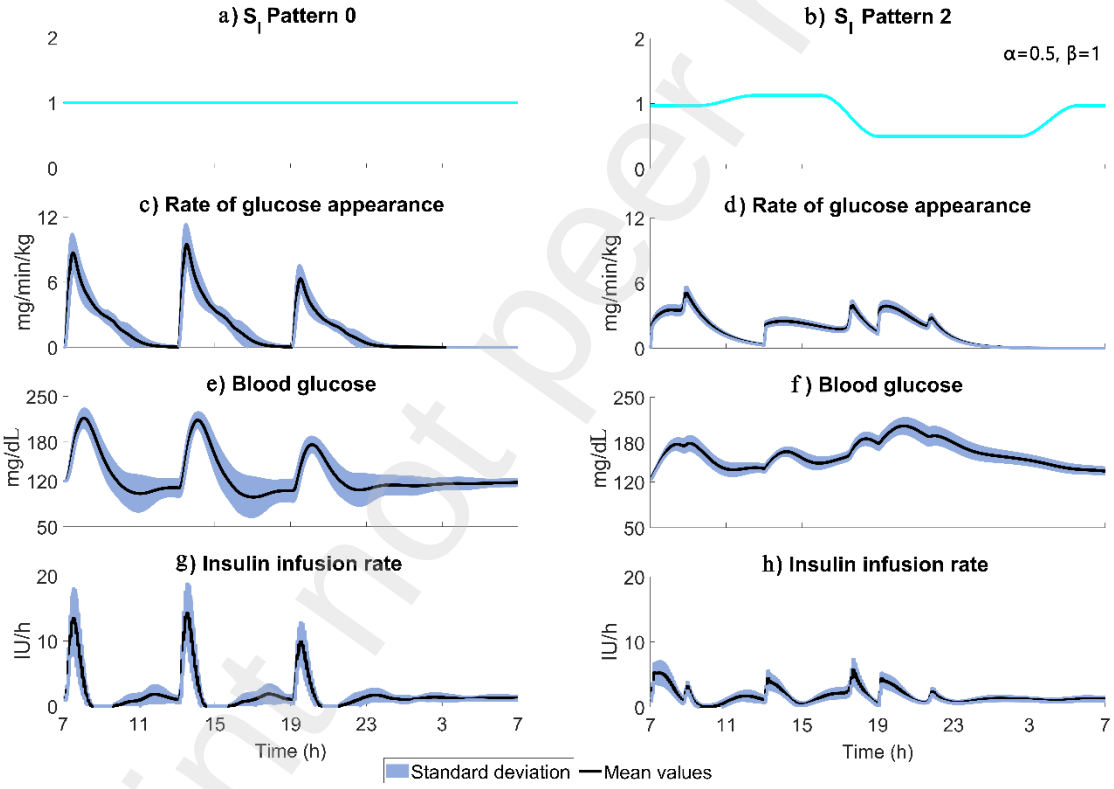

Figure 6 Simulation performance of two scenarios involving 10 adult virtual subjects with the same CLC therapy. Left, consolidated results from a test scenario with model-based R_a profiles and S_I pattern 0. Right, consolidated results from a test scenario with data-based R_a profiles and S_I pattern 2. **a)** and **b)** show the corresponding S_I pattern, **c)** and **d)** show the corresponding rate of glucose appearance, **e)** and **f)** show the corresponding blood glucose concentration, **g)** and **h)** show the corresponding insulin infusion rate. Blue shadow represents the standard deviation obtained

Overall, the results highlight the differences between version v1 and v2 incorporating realistic features regarding S_I and R_a. Results show that postprandial peaks obtained with the model-based

R_a profiles (v1) are significantly greater than those using the data-based R_a profiles (v2), 9.45 mg/min/kg vs. 5.05 mg/min/kg, respectively, see Figure 6 c) and 6 d).

In v2, a higher risk of hyperglycaemia was observed, especially for the third prandial event. Here, a BG of 185.37 mg/dL (attributed to the overlap of the independent profiles) was observed in the v2, whereas 175.89 mg/dL in the v1. Table 2 resumes several glycaemic indicators, revealing a greater risk of hypoglycaemia (LBGI) in the v1 simulation, in addition to a greater time above range (TAR), and a fewer time below range (TBR) and time in range (TIR). Marked differences are observed between both simulations, highlighting a higher average BG and lower interpatient variability for the v2 compared to the v1.

Table 2. Glycaemic indicators (mean ± standard deviation) obtained with the DT1-UAN simulator version v1 and v2 using the same CLC therapy

Variable	v1	v2	Absolute relative difference (%)
LBGI	0,84 ± 1,83	0,00 ± 0,00	100 ± 100
Average BG (mg/dL)	127,41 ± 13,15	162,44 ± 7,18	21,56 ± 83,15
Insulin infusion rate (IU/h)	1,8 ± 0,86	1,66 ± 0,49	1,87 ± 161,11
R_a (mg/min/kg)	1,63 ± 0,47	1,60 ± 0,18	1,87 ± 161,11
TAR (%)	14,51 ± 3,23	32,18 ± 11,71	54,91 ± 72,42
TIR (%)	82,28 ± 6,07	67,82 ± 11,71	21,32 ± 48,16
TBR (%)	3,2 ± 7,41	0,00 ± 0,00	100 ± 100

4. Discussion

4.1. A More Rigorous Validation for Glycaemic Control

The results of this study demonstrate that incorporating realistic intrapatient variability does not merely refine glycaemic outcomes but fundamentally alters the assessment of an insulin therapy's performance and robustness. The central finding is that simplified simulators, like the DT1-UAN v1, can mask significant clinical risks that only become apparent under more dynamic conditions. Our comparative in-silico trials (Figures 4-6) revealed that control strategies appearing adequate in a static environment can lead to adverse events, such as sustained hyperglycaemia or postprandial hypoglycaemia, when subjected to the variability introduced in the DT1-UAN v2. This finding underscores the critical importance of using realistic testbeds to avoid systematically biased conclusions about an algorithm's real-world efficacy.

The divergent outcomes are attributable to the distinct challenges posed by the two integrated features. The data-driven R_a profiles introduce high-frequency, unpredictable disturbances related to meal absorption, directly influencing postprandial control and immediate hypoglycaemia risk. In contrast, the stochastic S_I patterns introduce low-frequency, drifting changes in the patient's metabolic

state, testing a controller's ability to adapt over longer periods and prevent sustained glycaemic excursions. A truly robust CLC system must effectively handle both types of perturbations. The CLC controller used in this study served as a methodological probe to highlight this issue: its performance, nearly ideal in the simplified scenario, degraded when faced with combined R_a and S_I variability, revealing potential synchronization flaws. This confirms that the safety and efficacy of a control strategy are tightly coupled to the realism of its testing environment.

4.2. A Foundational Step Toward Digital Twins and Future Work

Beyond algorithm validation, the DT1-UAN v2 framework serves as a foundational step toward the development of clinically useful Digital Twins. As Cinar et al. [8] identify, therapy personalization is a key objective for which digital twins are the primary enabling technology. The relevance of our framework as a foundation for this next-generation technology is not merely theoretical. An effective Digital Twin must replicate an individual's unique stochastic variability (our S_I module) and their response to real-world perturbations (our R_a library). The value of these components is explicitly highlighted by the work of leading groups such as Colmegna et al. (2020), who utilized the data-driven meal library from our previous work [26] to challenge and validate their own virtual patient models [27]. Therefore, by formally integrating both of these critical variability sources into a unified platform, the modular architecture of DT1-UAN v2 provides a proven and robust foundation upon which future personalized digital twins can be built.

Future work will focus on enhancing this physiological fidelity and clinical applicability. Key limitations to be addressed include expanding the inter- and intrapatient variability by allowing dynamic transitions between S_I patterns and incorporating individual modulation of meal absorption dynamics. Further development will also involve strengthening the open-loop therapy simulation with logic-based bolus adjustment recommendations and pursuing formal clinical validation of the simulator against data from PWT1D cohorts. Finally, improving the framework's usability with a cross-platform user interface and expanding the meal library to reflect diverse nutritional patterns will broaden its applicability in clinical, academic, and educational contexts, including its potential integration with AI tools for predictive modelling and decision support [33-37]. These advancements will continue to accelerate the path toward safer and more effective personalized therapies for T1D.

5. Conclusions

This study introduces and evaluates a novel enhanced T1D simulation framework that integrates stochastic insulin sensitivity patterns and data-driven meal profiles to better represent the metabolic variability of daily life. Through the parametrisation of S_I and R_a in the DT1-UAN v2 simulator, the framework supports therapeutic assessments under more realistic scenarios.

Conventional, simplified simulators can mask significant clinical risks, such as postprandial hypoglycaemia or poor controller synchronization, and may lead to overly optimistic assessments of an algorithm's performance. In contrast, introducing variability in R_a and S_I exposes potential synchronisation issues that can impact glycaemic control [38].

Ultimately, this work provides a valuable tool to support the design and validation of safer, precise, adaptive, and effective strategies for managing type 1 diabetes. By providing a platform to stress-test algorithms against real-world variability, this work accelerates the path toward truly personalized therapy systems and the realization of effective digital twins for diabetes management.

Appendix A

Glucose Subsystem

$$\dot{G_p} = EGP(G_p,I_d,H_d) + R_a - U_{ii} - E(G_p) - k_1 G_p + k_2 G_t \quad \text{(A.1)}$$

$$\dot{G_t} = -U_{id}(G_p,G_t,X) + k_1 G_p - k_2 G_t \quad \text{(A.2)}$$

$$G = \frac{G_p}{V_G} \quad \text{(A.3)}$$

Insulin Subsystem

$$\dot{X_{il}} = \begin{bmatrix} -(m_2+m_4) & m_1 \\ m_2 & -(m_1+m_3) \end{bmatrix} X_{il} + \begin{bmatrix} 1 \\ 0 \end{bmatrix} R_{ai}(t) \quad X_{il} = \begin{bmatrix} I_p \\ I_l \end{bmatrix} \quad \text{(A.4)}$$

$$I(t) = \begin{bmatrix} \frac{1}{V_i} & 0 \end{bmatrix} X_{il} \quad X_{il}(0) = \begin{bmatrix} I_{pb} \\ I_{lb} \end{bmatrix} \quad \text{(A.5)}$$

Ingested Glucose

$$C_a(t) = \frac{D}{\Delta T_m}(u(t - T_m) - u(t - (T_m + \Delta T_m))) \quad \text{(A.6)}$$

Oral Absorption Model

$$Q_{sto} = Q_{sto1} + Q_{sto2} \quad \text{(A.7)}$$

$$\dot{Q_{sto1}} = -k_{gri} Q_{sto1} + IG(t) \qquad Q_{sto1}(0) = 0 \quad \text{(A.8)}$$

$$\dot{Q_{sto2}} = -k_{emp}(Q_{sto}) Q_{sto2} + k_{gri} Q_{sto1} \qquad Q_{sto2}(0) = 0 \quad \text{(A.9)}$$

$$\dot{Q_{gut}} = -k_{abs} Q_{gut} + k_{emp}(Q_{sto}) Q_{sto2} \qquad Q_{gut}(0) = 0 \quad \text{(A.10)}$$

$$R_a(t) = \frac{f k_{abs} Q_{gut}}{BW} \quad \text{(A.11)}$$

September 5, 2025

$$k_{emp}(Q_{sto}) = \begin{cases} k_{min} + \dfrac{k_{max} - k_{min}}{2} k_e(Q_{sto}) & D_n > D_{th} \\ \dfrac{D_{th}}{D_n}\left(k_{min} + \dfrac{k_{max} - k_{min}}{2} k_e(Q_{sto})\right) & D_n \le D_{th} \end{cases} \quad \text{(A.12)}$$

$$k_e = \tanh(\alpha(Q_{sto} - bD_n)) - \tanh(\beta(Q_{sto} - cD_n)) + 2 \quad \text{(A.13)}$$

$$D_n = D + Q_{sto}(T_m) \quad \text{(A.14)}$$

Glucagon Kinetics and Secretion

$$\dot{H}(t) = -nH + SR_H \qquad H(0) = H_b \quad \text{(A.15)}$$

$$SR_H = SR_H^d(G_p, G_t, I_d, H_d) + SR_H^s \quad \text{(A.16)}$$

$$SR_H^d(G_p, G_t, I_d, H_d) = \delta \max\left(-\frac{\dot{G}_p}{V_g}, 0\right) \quad \text{(A.17)}$$

$$\dot{SR}_H^s = -\rho SR_H^s + \rho GSR_H(G, I) \quad \text{(A.18)}$$

$$GSR_H(G, I) = \begin{cases} \max\left(\dfrac{\sigma(G_{th} - G)}{I - I_{th} + 1} + SR_h^b, 0\right) & if \quad I \ge I_{th} \\ max(\sigma(G_{th} - G) + SR_h^b, 0) & if \quad I < I_{th} \end{cases} \quad \text{(A.19)}$$

Endogenous Glucose Production

$$\dot{I}_d = -k_i(I_d - I_i) \qquad I_d(0) = I_b \quad \text{(A.20)}$$

$$\dot{I}_1 = -k_i(I_1 - I) \qquad I_1(0) = I_b \quad \text{(A.21)}$$

$$\dot{H}_d = -k_h H_d + k_h max((H - H_b), 0) \qquad H_d(0) = 0 \quad \text{(A.22)}$$

$$EGP(G_p, I_d, H_d) = \max(k_{p1} - k_{p2}G_p - k_{p3}I_d + \varepsilon H_d, 0) \quad \text{(A.23)}$$

Glucose Utilization

$$\dot{X} = -p_{2u}X + P_{2u}(I - I_b) \qquad X(0) = 0 \quad \text{(A.24)}$$

$$U_{ii} = F_{cns} \quad \text{(A.25)}$$

$$U_{id}(G_p, G_t, X) = \frac{K_m(G_p, X)G_t}{K_{mo} + G_t} \quad \text{(A.26)}$$

$$K_m(G_p,X) = [V_{m0} + V_{mx}(1 + r_1 risk(G))X] \quad \text{(A.27)}$$

$$risk(G) = \begin{cases} 0 & if, G \geq G_b \\ 10\left(ln^{r2}\left(\frac{G}{G_b}\right)\right)^2 & if, G_{th} \leq G \leq G_b \\ 10\left(ln^{r2}\left(\frac{G_{th}}{G_b}\right)\right)^2 & if\ G < G_{th} \end{cases} \quad \text{(A.28)}$$

Renal Excretion

$$E(G_p) = \begin{cases} k_{e1}(G_p - k_{e2}) & if, G_p > k_{e2} \\ 0 & if, G_p \leq k_{e2} \end{cases} \quad \text{(A.29)}$$

Subcutaneous Insulin Kinetics

$$\dot{X}_{sci} = \begin{bmatrix} -(k_d + k_{a1}) & 0 \\ k_d & -k_{a2} \end{bmatrix} X_{sci} + \begin{bmatrix} 1 \\ 0 \end{bmatrix} IIR(t) \qquad X_{sci} = \begin{bmatrix} I_{sc1} \\ I_{sc2} \end{bmatrix} \quad \text{(A.30)}$$

$$R_{ai}(t) = [k_{a1} \quad k_{a2}] X_{sci} \qquad X_{sci}(0) = \begin{bmatrix} I_{sc1ss} \\ I_{sc2ss} \end{bmatrix} \quad \text{(A.31)}$$

Subcutaneous Glucose Kinetics

$$\dot{G}_s(t) = -\frac{1}{T_s}\ G_s(t) + \frac{1}{T_s}\ G_p(t) \qquad G_s(0) = G_{pb} \quad \text{(A.32)}$$

References

[1] Diabetes Control and Complications Trial Research Group, D M Nathan, S Genuth, et al (1993) The effect of intensive treatment of diabetes on the development and progression of long-term complications in insulin-dependent diabetes mellitus. N Engl J Med 329:977–986. https://doi.org/10.1056/NEJM199309303291401

[2] Gómez AM, Vallejo S, Ardila F, et al (2018) Impact of a Basal-Bolus Insulin Regimen on Metabolic Control and Risk of Hypoglycemia in Patients With Diabetes Undergoing Peritoneal Dialysis. J Diabetes Sci Technol 12:129–135. doi: 10.1177/1932296817730376.

[3] Dovc K, Battelino T (2020) Evolution of Diabetes Technology. Endocrinol Metab Clin North Am 49:1–18. https://doi.org/10.1016/J.ECL.2019.10.009

[4] Rodríguez-Sarmiento DL, León-Vargas F, García-Jaramillo M (2022) Artificial pancreas systems: experiences from concept to commercialisation. Expert Rev Med Devices 19:877–894. https://doi.org/10.1080/17434440.2022.2150546

[5] Gómez AM, Henao DC, Taboada LB, et al (2019) Impact of sensor-augmented pump therapy with predictive low-glucose management on hypoglycemia and glycemic control in patients with type 1 diabetes mellitus: 1-year follow-up. Diabetes Metab Syndr 13:2625–2631. https://doi.org/10.1016/J.DSX.2019.07.024

[6] León-Vargas F, Arango Oviedo JA, Luna Wandurraga HJ (2022) Two Decades of Research in Artificial Pancreas: Insights from a Bibliometric Analysis. J Diabetes Sci Technol 16:434–445.

https://doi.org/10.1177/19322968211005500
[7] Biester T, Tauschmann M, Chobot A, et al (2022) The automated pancreas: A review of technologies and clinical practice. Diabetes Obes Metab 24 Suppl 1:43–57. https://doi.org/10.1111/DOM.14576
[8] Cinar A, Basu A, Bequette BW, et al (2025) Metabolic Models, in Silico Trials, and Algorithms. J Diabetes Sci Technol 19:895–907. https://doi.org/10.1177/19322968251338300
[9] Quiroz G (2019) The evolution of control algorithms in artificial pancreas: A historical perspective. Annu Rev Control 48:222–232. https://doi.org/10.1016/J.ARCONTROL.2019.07.004
[10] Cobelli C, Kovatchev B (2023) Developing the UVA/Padova Type 1 Diabetes Simulator: Modeling, Validation, Refinements, and Utility. J Diabetes Sci Technol 17:1493–1505. https://doi.org/10.1177/19322968231195081
[11] Dalla Man C, Micheletto F, Lv D, et al (2014) The UVA/PADOVA Type 1 Diabetes Simulator: New Features. J Diabetes Sci Technol 8:26–34. https://doi.org/10.1177/1932296813514502
[12] Molano-Jimenez A, Leon-Vargas F (2017) UVa/Padova T1DMS dynamic model revision: For embedded model control. 2017 IEEE 3rd Colombian Conference on Automatic Control, CCAC 2017 - Conference Proceedings 2018-January:1–6. https://doi.org/10.1109/CCAC.2017.8276390
[13] Leon-Vargas F, Jutinico AL, Molano-Jimenez A (2021) Hypoglycemia Prevention Using an Embedded Model Control with a Safety Scheme: In-silico Test. Advances in Intelligent Systems and Computing 1240 AISC:186–196. https://doi.org/10.1007/978-3-030-54568-0_19
[14] Gamez Peña, Y. (2022). Evaluación de controladores PID para el control de glucemia de pacientes con diabetes tipo 1 a partir de sincronizaciones mediante el método LAMBDA. (Trabajo de grado) Universidad Antonio Nariño.
[15] D. L. Rodríguez-Sarmiento, León-Vargas F, Garelli F (2022) Practical constraint definition in safety schemes for artificial pancreas systems. Int J Artif Organs 45:535–542. https://doi.org/10.1177/03913988221095586
[16] Rodríguez-Sarmiento DL (2023) Diseño y evaluación de algoritmos de análisis de desempeño y control para sistemas de administración automática de insulina en pacientes con diabetes (PhD Thesis). Universidad Antonio Nariño.
[17] Rodríguez-Sarmiento DL, Jutinico AL, León-Vargas F (2024) A constrained robust Markovian control approach with robust Kalman filter for fully automated insulin delivery systems. Biomed Signal Process Control 93:106166. https://doi.org/10.1016/J.BSPC.2024.106166
[18] Villa-Tamayo MF, Leon-Vargas F, Garcia-Jaramillo M, Rivadeneira PS (2021) Glycemic Control Strategy Based on an Impulsive MPC With Safety Layer Coupling for IOB Limitation. IEEE Control Systems Letters, 5:1669-1674. doi: 10.1109/LCSYS.2020.3042651
[19] Schiavon M, Dalla Man C, Kudva YC, et al (2014) Quantitative estimation of insulin sensitivity in type 1 diabetic subjects wearing a sensor-augmented insulin pump. Diabetes Care 37:1216–1223. https://doi.org/10.2337/DC13-1120
[20] Visentin R, Dalla Man C, Kudva YC, et al (2015) Circadian variability of insulin sensitivity: physiological input for in silico artificial pancreas. Diabetes Technol Ther 17:1–7. https://doi.org/10.1089/DIA.2014.0192
[21] Estremera E, Cabrera A, Beneyto A, Vehi J (2022) A simulator with realistic and challenging scenarios for virtual T1D patients undergoing CSII and MDI therapy. J Biomed Inform 132:. https://doi.org/10.1016/J.JBI.2022.104141
[22] Herrero P, Bondia J, Palerm CC, et al (2012) A simple robust method for estimating the glucose rate of appearance from mixed meals. J Diabetes Sci Technol 6:153–162. https://doi.org/10.1177/193229681200600119
[23] Visentin R, Man CD, Cobelli C (2016) One-Day Bayesian Cloning of Type 1 Diabetes Subjects: Toward a Single-Day UVA/Padova Type 1 Diabetes Simulator. IEEE Trans Biomed Eng 63:2416–2424. https://doi.org/10.1109/TBME.2016.2535241
[24] Dalla Man C, Rizza RA, Cobelli C (2007) Meal simulation model of the glucose-insulin system. IEEE

Trans Biomed Eng 54:1740–1749. https://doi.org/10.1109/TBME.2007.893506
[25] Camerlingo N, Vettoretti M, Del Favero S, et al (2021) Mathematical Models of Meal Amount and Timing Variability With Implementation in the Type-1 Diabetes Patient Decision Simulator. J Diabetes Sci Technol 15:346–359. https://doi.org/10.1177/1932296820952123
[26] León-Vargas, F. (2013). Design and implementation of a closed-loop blood glucose control system in patients with type 1 diabetes (PhD Thesis). Universitat de Girona.
[27] Colmegna, P., et al. (2020). Mapping data to virtual patients in type 1 diabetes. Control Engineering Practice, 103, 104605.
[28] Visentin R, Campos-Náñez E, Schiavon M, et al (2018) The UVA/Padova Type 1 Diabetes Simulator Goes From Single Meal to Single Day. J Diabetes Sci Technol 12:273–281. https://doi.org/10.1177/1932296818757747
[29] C. Barajas-Solano JBRCPH y JV (2012) A review of absorption models for mixed meals. In 5th International Conference on Advanced Technologies and Treatments for Diabetes, Barcelona, Spain
[30] Zafar MI, Mills KE, Zheng J, et al (2019) Low-glycemic index diets as an intervention for diabetes: a systematic review and meta-analysis. Am J Clin Nutr 110:891–902. https://doi.org/10.1093/AJCN/NQZ149
[31] Rodríguez-Sarmiento X (2023) Implementación de variabilidad paramétrica intrapaciente y una librería de comidas mixtas para la simulación realista de pacientes con diabetes tipo 1 (Trabajo de grado) Universidad Antonio Nariño.
[32] Colmegna P, Sánchez-Peña RS, Gondhalekar R (2016) Control-oriented linear parameter-varying model for glucose control in type 1 diabetes. 2016 IEEE Conference on Control Applications, CCA 2016 410–415. https://doi.org/10.1109/CCA.2016.7587865
[33] Riddell MC, Gallen IW, Smart CE, et al (2017) Exercise management in type 1 diabetes: a consensus statement. Lancet Diabetes Endocrinol 5:377–390. https://doi.org/10.1016/S2213-8587(17)30014-1
[34] Dejournett L, Dejournett J (2016) In Silico Testing of an Artificial-Intelligence-Based Artificial Pancreas Designed for Use in the Intensive Care Unit Setting. J Diabetes Sci Technol 10:1360. https://doi.org/10.1177/1932296816653967
[35] Rodríguez-Sarmiento DL, Suárez Méndez AF, Murcia Doncel MP, et al (2024) Mejoramiento de la calidad de vida a través del apoyo integral a la gestión de la diabetes por medio de investigación científica e ingeniería traslacional. Perspectivas multidisciplinares en salud: estrategias prácticas para el bienestar, 2024, ISBN 978-84-09-63623-5, p109-116
[36] Chung WK, Erion K, Florez JC, et al (2020) Precision medicine in diabetes: a consensus report from the American Diabetes Association (ADA) and the European Association for the Study of Diabetes (EASD). Diabetologia 63:1671. https://doi.org/10.1007/S00125-020-05181-W
[37] Murpy M (2024) Artificial Intelligence in Diabetes Management: Transforming Care through Technology. J Diabetes Med Care 7(5):266–268. https://doi.org/10.37532/JDMC.2024.7(5).266-268.
[38] Nefs G (2022) The Psychological Implications of Automated Insulin Delivery Systems in Type 1 Diabetes Care. Frontiers in clinical diabetes and healthcare 3:. https://doi.org/10.3389/FCDHC.2022.846162

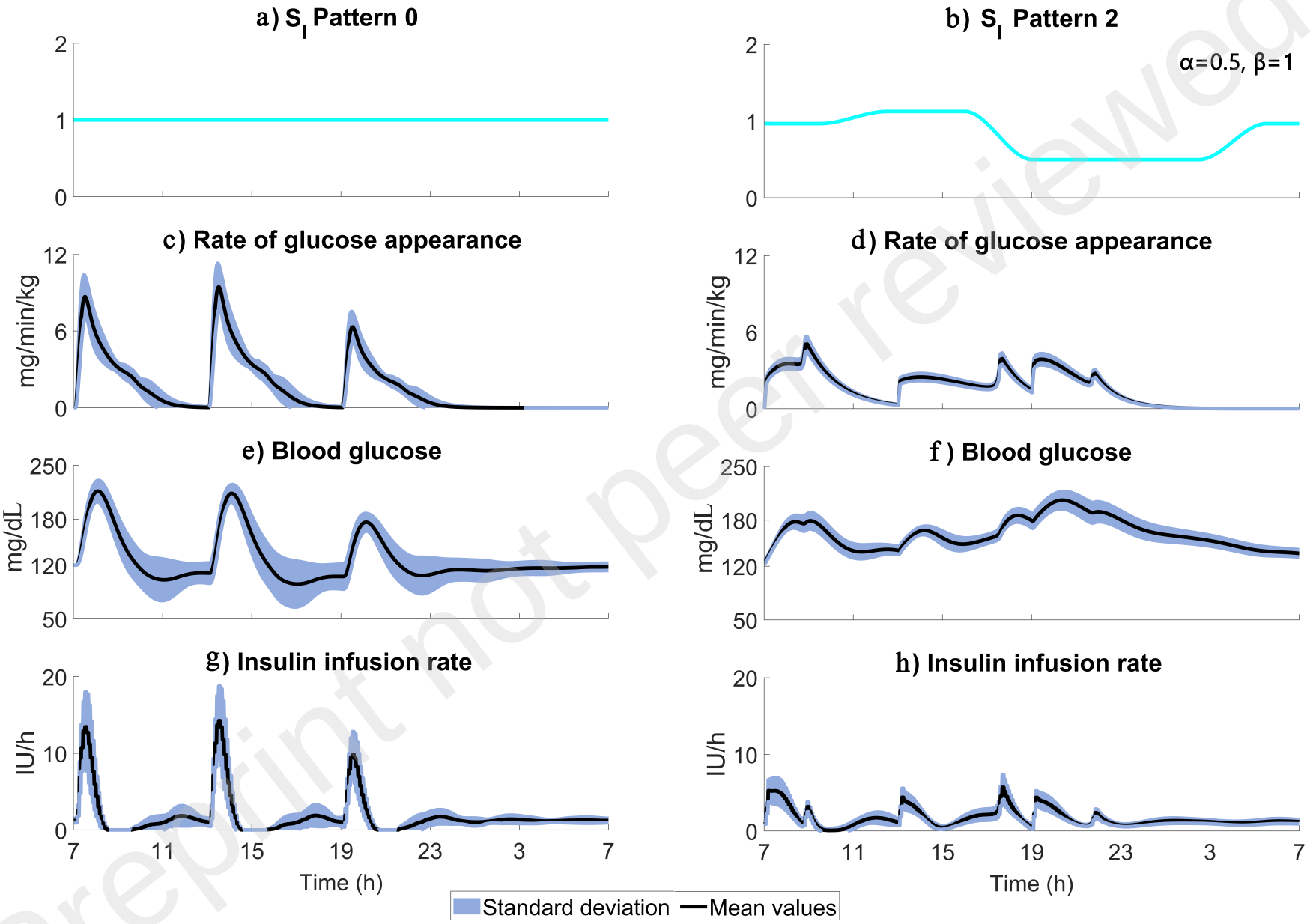

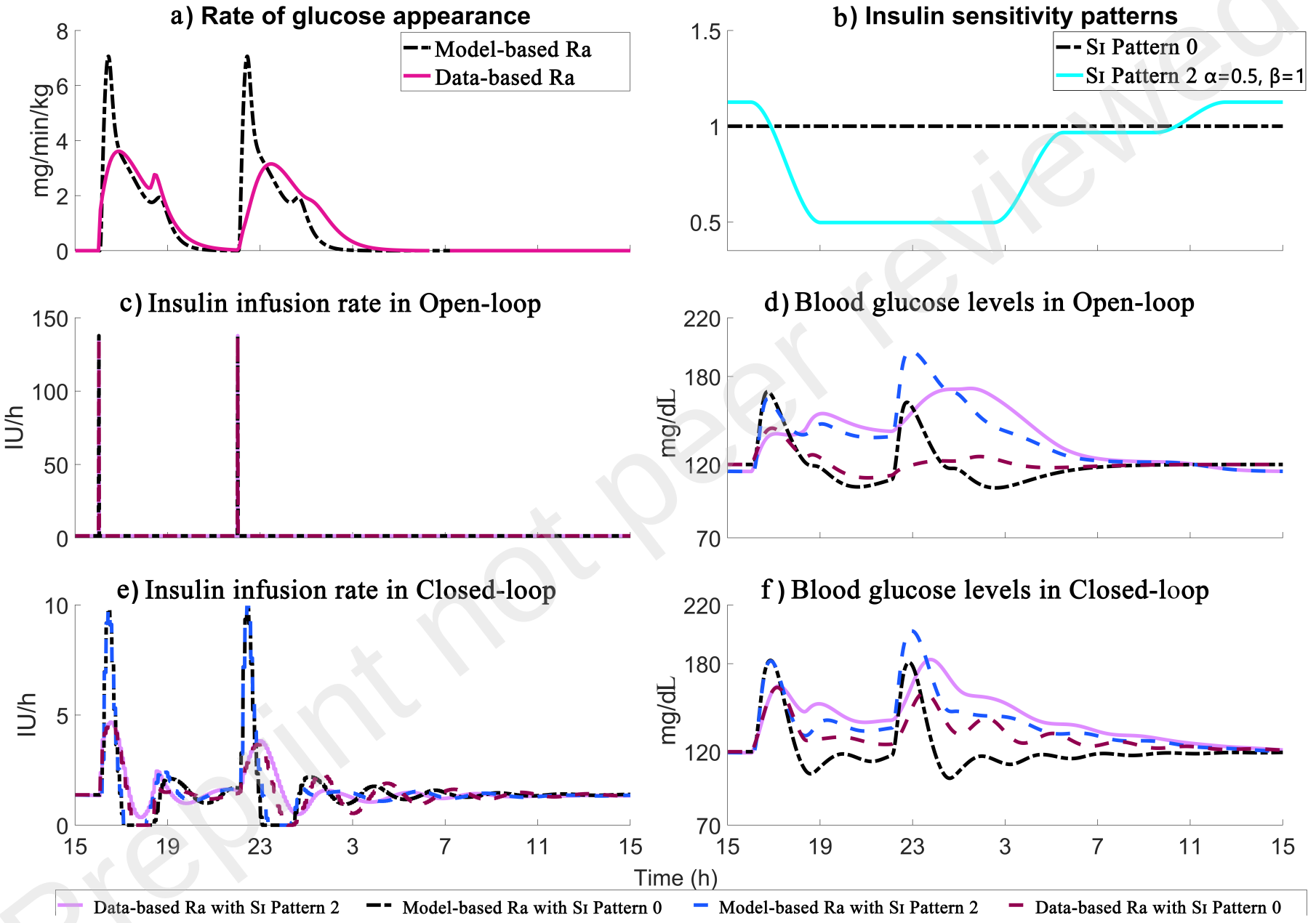

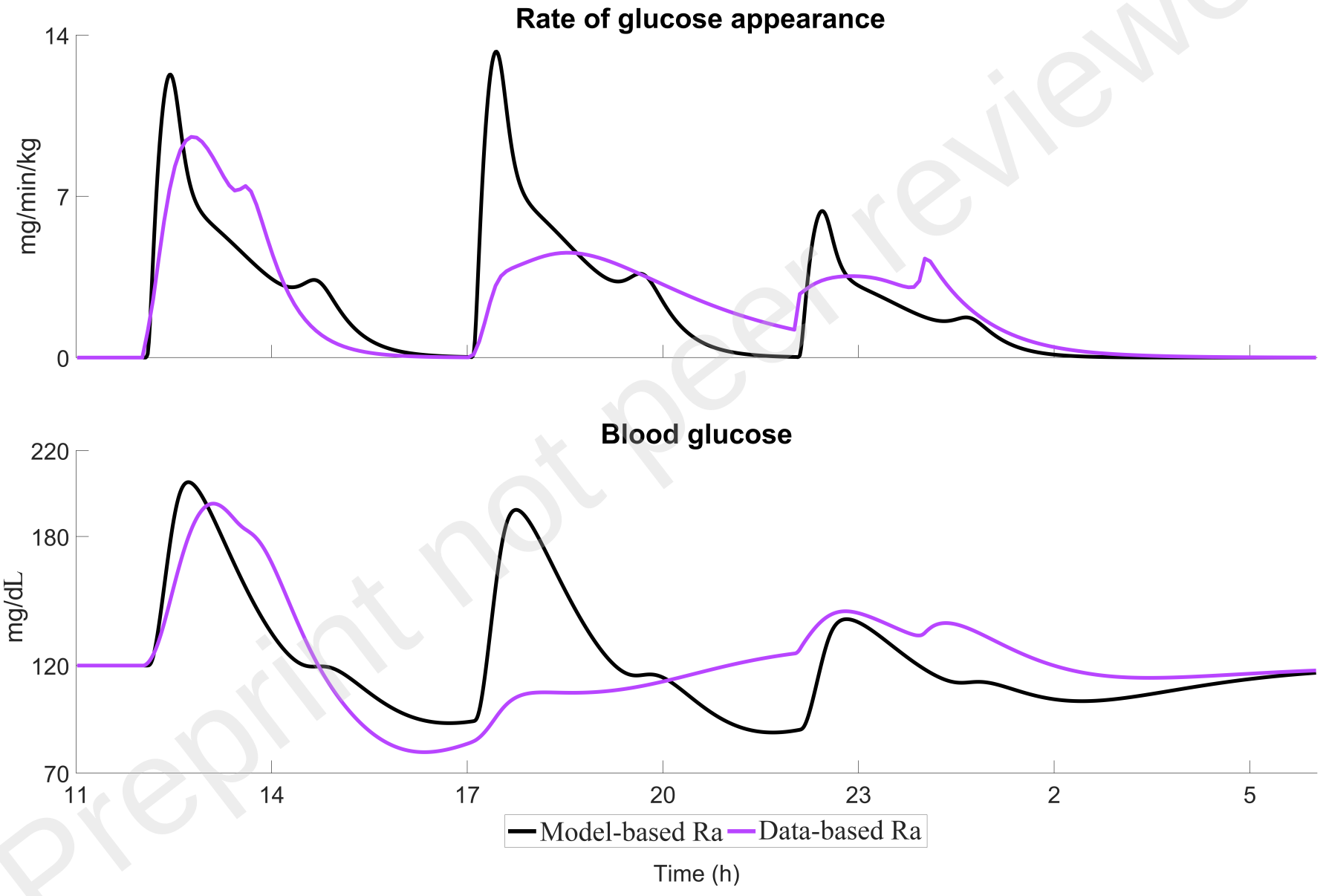

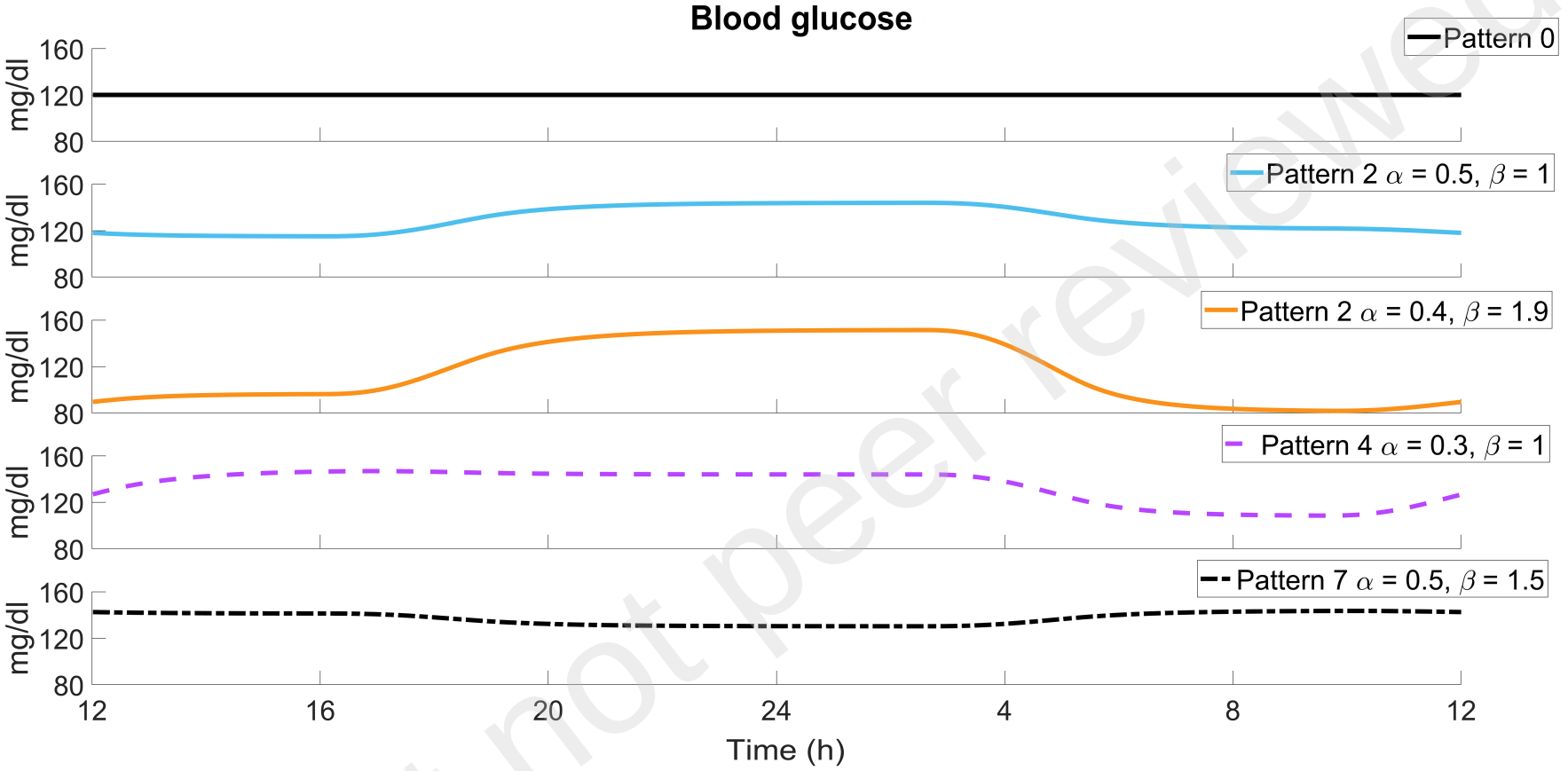

a)

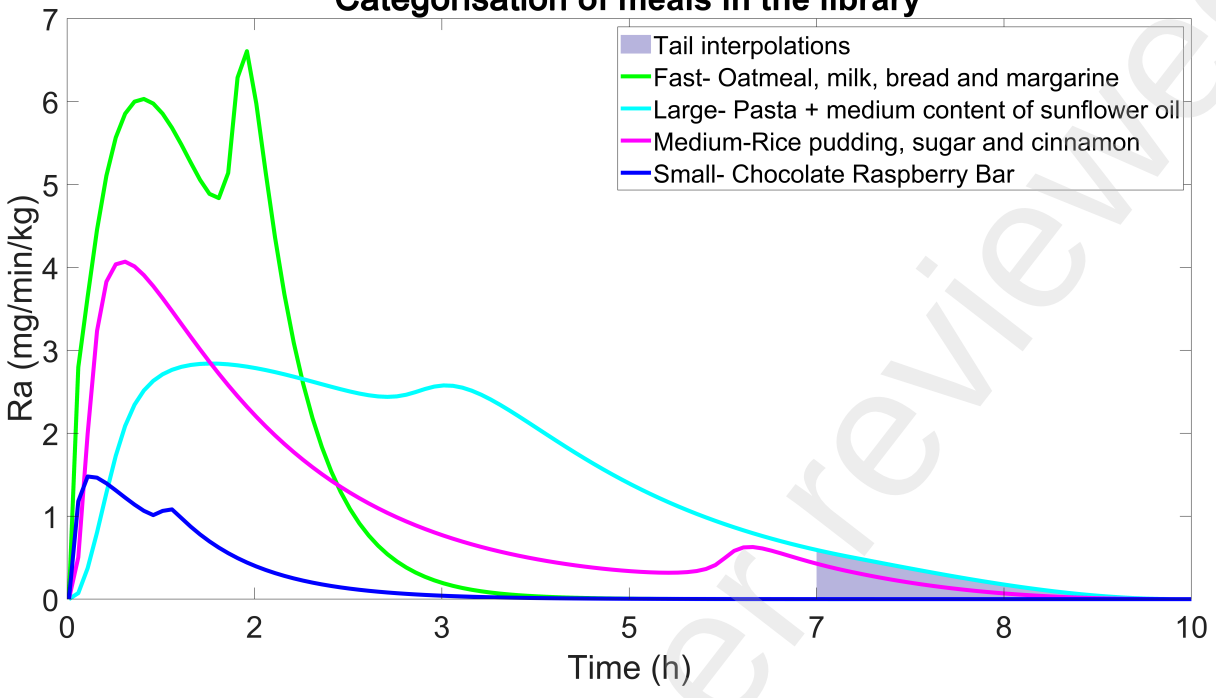

b)